УДК 539.143 https://doi.org/10.15407/jnpae2023.04.306

A. H. Taqi*, G. A. Mohammed

Department of Physics, College of Science, Kirkuk University, Kirkuk, Iraq

*Corresponding author: alitaqi@uokirkuk.edu.iq

ISOSCALAR MONOPOLE RESPONSE IN THE NEUTRON-RICH MOLYBDENUM ISOTOPES USING SELF-CONSISTENT QRPA

The isoscalar giant monopole resonance (ISGMR) of even molybdenum isotopes ^{92,94,96,98,100}Mo has been studied within the Skyrme self-consistent Hartree - Fock - Bardeen, Cooper, and Schrieffer and quasi-particle random phase approximation. Ten sets of Skyrme-type interactions of different values of the nuclear matter incompressibility coefficient K_{NM} are used in the calculations. The calculated strength distributions, centroid energies E_{cen}, scaled energies E_s and constrained energies E_{con} of ISGMR are compared with available experimental data. Due to the appropriate value of the nuclear matter incompressibility K_{NM}, several types of Skyrme interactions were successful in describing the ISGMR strength distribution in the ^{92,94,96,98,100}Mo isotopes. As a result, high correlations between E_{cen} and K_{NM} were found.

Keywords: strength distribution, Skyrme force, Hartree - Fock - Bardeen - Cooper - Schrieffer, quasiparticle random phase approximation.

1. Introduction

To represent collective modes like giant resonances (GR), microscopic models based on the self-consistent Hartree - Fock (HF) and random phase approximation (RPA) are appropriate [1]. The quasiparticle random phase approximation (QRPA), based on the Hartree - Fock + Bardeen, Cooper, and Schrieffer (HF+BCS) model, is an enhanced RPA model that considers the pairing effect, which is anticipated to be significant for open-shell nuclei. This enables us to examine the entire nuclear chart's nuclear structure.

The self-consistency QRPA model with Skyrme effective interaction [2] has been successful in describing low-lying collective states of oxygen [3], sulfur, and argon [4] isotopes. However, the BCS approximation cannot properly describe the pairing correlation of many neutron-rich nuclei along the drip-line nuclei [5], as a result, various strategies have been devised, including the Hartree - Fock - Bogoliubov (HFB) theory [6] and the continuum QRPA equations derived from the time-dependent-HFB theory [7, 8].

Measurements of GR have yielded an abundance of new information about nuclear structure and magicity [9], as well as helped clarify another important problem related to nuclear incompressibility [10], where our understanding of nuclear incompressibility is incomplete. In other words, it appears challenging to identify a model that may provide a thorough description of the isoscalar giant monopole resonance (ISGMR), especially in light of recent information on isotopic chains, including open-shell systems and neutron-rich nuclei [11 - 14]. This can be seen in the recent theoretical works on the subject [15 - 20].

Evaluating the ISGMR of neutron-rich and exotic nuclei is crucial to improving our understanding of nuclear incompressibility and nuclear magicity. Several relativistic and nonrelativistic models have predicted a soft monopole mode in neutron-rich nuclei of about 14 MeV [21 - 23], but it has never been observed in nuclei far from stability, due to the difficulty in measuring. The non-collective nature of the soft monopole mode is expected, and its detection could provide important insights into spin-orbit splitting [24]. Therefore, it is crucial to evaluate the isoscalars (protons and neutrons moving in phase) monopole response in neutron-rich nuclei.

The energy $E_{GMR} = \left(\hbar^2 K_A / m\left\langle r^2\right\rangle\right)^{1/2}$ is inversely correlated with the mean square nuclear radius and directly correlated with the incompressibility K_A of the nucleus. Using the $A^{1/3}$ expansion of K_A, one can then try to directly extract the different coefficients of the expansion equation from experimental data. The comparison between this expansion and the corresponding calculated incompressibility could give some information on the incompressibility of nuclear matter K_{NM} and the features of the effective interaction.

Understanding the behavior of stars and heavy-ion processes requires knowledge of the K_{NM}. However, it is common practice to determine K_{NM} by performing microscopic E_{GMR} calculations [25 - 28] by comparing the results with the experimental values of E_{GMR} and studying its sensitivity to the value of K_{NM} associated with the effective interaction. In 1999, $K_{\mathrm{NM}} = 231 \pm 5$ MeV was determined by comparing observations of the ISGMRs for ^{40}Ca, ^{90}Zr, ^{116}Sn, ^{144}Sm, and ^{208}Pb [29] to HF-based RPA calculations that employed the Gogny interaction [26] and took pairing and harmonicity corrections into account. When compared to data from the 1970s and 1980s, these data were of significantly higher quality (for a summary of these data, see Ref. [30]) which had been previously used to extract nuclear incompressibility. The effect of incompressibility modulus K_{NM} and symmetry energy density J on charge distribution and root-mean-square radii of neutron R_{n} and proton R_{p} have been investigated for light, medium, and heavy closed-shell nuclei ^{40}Ca, ^{48}Ca, ^{90}Zr, ^{116}Sn, ^{144}Sn, and ^{208}Pb within the framework of self-consistent HF with 20 types of Skyrme interactions [31].

There are 33 known isotopes of molybdenum ($Z = 42$), with atomic masses ranging from 83 to 115, as well as four metastable nuclear isomers. Seven isotopes with atomic masses of 92, 94, 95, 96, 97, 98, and 100 are found in nature. Molybdenum's unstable isotopes all undergo isotopic decay to form ruthenium, technetium, zirconium, and niobium. The sole unstable naturally occurring isotope is ^{100}Mo, which has a half-life of about $1 \cdot 10^{19}$ years, and double beta decays into ^{100}Ru [32].

Moalem et al. were the first to notice isoscalar GR in the Mo isotopes, and they used an inelastic scattering of 110 MeV ^{3}He to pinpoint the giant quadrupole resonance (GQR) in all stable Mo isotopes [33]. The GQR and GMR in ^{92}Mo were examined by Duhamel et al. [34] using inelastic scattering of 152 MeV particles. Youngblood et al. used an inelastic scattering of 240 MeV particles at small angles, including 0°, to investigate the isoscalar GR in ^{90,92,94}Zr and ^{92,96,98,100}Mo [35 - 37]. According to Ref. [35], the E0 strength distribution of these Zr and Mo isotopes revealed high and low-energy components separated by 7 - 9 MeV.

A comparison between the experimental results of ISGMR for open-shell nuclei near $A = 90$ with relativistic self-consistent RPA calculations indicates that the ISGMR response begins to show softness in the molybdenum isotopes beginning with $A = 92$ [38]. Colò et al. analyzed the experimental data on the ISGMR and ISGQR in ^{92,94,96,98,100}Mo within a fully self-consistent QRPA approach with the Skyrme sets SkM*, SLy6, SVbas, and SkP$^{\delta}$ of different values of nuclear matter incompressibility (K_{MN}: 234, 230, 217, and 202 MeV), respectively [39].

In this study, we use the Skyrme QRPA method based on HF- Bardeen - Cooper - Schrieffer (HF+BCS) to examine the strength distribution of the ISGMR in the ^{92,94,96,98,100}Mo isotopes. Having a large number of Skyrme-force parameterizations requires a continuous search for the best for describing the experimental data. Therefore, ten sets of Skyrme interactions were used: KDE0v1 [40], eMSL08 [41], SKX [42], SGOI [43], v080 [44], SKP [45], SIV [46], SIII [47], SKIII [48], and SGI [43] with a wide range of K_{NM} values starting at 200 MeV and ending at 361 MeV, that does not account for previous works [38, 39]. The calculated strength distributions, centroid energy, constrained energy, and scaling energy are compared with available experimental data. As well, the calculated values of the centroid energies were supported by statistical calculations by determining and discussing the statistical linear Pearson coefficient.

2. Formalism

The Skyrme effective interaction (of parameters $t_0.\ t_1.\ t_2.\ t_3.\ x_0.\ x_1.\ x_2.\ x_3,$ Wo and α) is one of the most convenient forces used in HF calculations [49 - 51]:

$$V(r_1,r_2) = t_0(1+x_0P_\sigma)\delta(r_1 - r_2) +$$
$$+\frac{1}{2}t_1\left(1+x_1P_{12}^{\alpha}\right)\cdot\left[\overleftarrow{k}_{12}^2\delta(r_1-r_2)+\delta(r_1-r_2)\vec{k}_{12}^2\right]+$$
$$+t_2\left(1+x_2P_{12}^{\alpha}\right)\overleftarrow{k}_{12}\delta(r_1-r_2)\vec{k}_{12}+$$
$$+\frac{1}{6}t_3\left(1+x_3P_{12}^{\alpha}\right)\rho^{\alpha}(R)\delta(r_1-r_2)+$$
$$+i\,W_0\overleftarrow{k}_{12}\delta(r_1-r_2)(\vec{\sigma}_1+\vec{\sigma}_2)\,\vec{k}_{12}, \qquad (1)$$

where $\vec{\sigma}_i$ is the Pauli spin operator, $\vec{k}_{12} = -\frac{i\left(\overleftarrow{\nabla}_1-\overleftarrow{\nabla}_2\right)}{2}$, P_{12}^{α} is the spin-exchange operator.

The variational principle can be used to determine the total energy E of HF equations based on Skyrme's interaction as a product of single-particle functions φ [52, 53]

$$\left\langle \delta\varphi \middle| H(r) \middle| \varphi \right\rangle = 0. \qquad (2)$$

The HF equations are coupled to the standard BCS equations, that in spherical symmetry the particle number n with $a = (n, l, j)$ read as

$$n = \sum_a (2j_a + 1)v_a^2, \qquad (3)$$

and gap equation Δ_a,

$$\Delta_a = -\sum_b \frac{\Delta_b}{2E_b} V_{a\tilde{a}b\tilde{b}}, \tag{4}$$

where the tilde designates the time-reversal state, and E and v are the typical quasi-particle energies and BCS amplitudes, respectively [54]. A zero-range, density-dependent pairing forces are used to calculate the matrix elements $V_{a\tilde{a}b\tilde{b}}$.

The total HF-BCS energy can be calculated directly from the force, or energy functional

$$E = E_{\text{KE}} + E_{\text{Skyrme}} + E_{\text{Coul}} + E_{\text{Pair}}, \tag{5}$$

where E_{KE}, E_{Skyrme}, E_{Coul}, and E_{Pair} are the Kinetic, Skyrme, Coulomb, and Pair contributions to the energy, respectively. The equations of E_{KE} and E_{Skyrme} are given in Refs. [55, 56]. The E_{Coul} has direct and exchange parts. The E_{Pair} can be found in Ref. [56].

Based on the HF+BCS ground state, the ν-th excited state E_x^{ν} can be calculated within the QRPA model. The compact form of QRPA equations can be written as follows [54, 57]:

$$\begin{pmatrix} A_{ab,cd} & B_{ab,cd} \\ -B^*_{ab,cd} & -A^*_{ab,cd} \end{pmatrix} \begin{pmatrix} X^{\nu}_{cd} \\ Y^{\nu}_{cd} \end{pmatrix} = E_x^{\nu} \begin{pmatrix} X^{\nu}_{ab} \\ Y^{\nu}_{ab} \end{pmatrix}, \tag{6}$$

where X^{ν} and Y^{ν} are the corresponding amplitudes. The matrices A and B on the HF-BCS two-quasiparticle bases have the form

$$A_{ab,cd} = (1+\delta_{ab})^{-\frac{1}{2}} (1+\delta_{cd})^{-\frac{1}{2}} \cdot [(E_a + E_b)\delta_{ac}\delta_{bd} + (u_a u_b u_c u_d + v_a v_b v_c v_d) G(abcd;J) +$$

$$+ (u_a v_b u_c v_d + v_a u_b v_c u_d) F(abcd;J) - (-1)^{j_c + j_d - J'} (u_a v_b v_c u_d + v_a u_b u_c v_d) F(abdc;J)], \tag{7}$$

$$B_{ab,cd} = (1+\delta_{ab})^{-\frac{1}{2}} (1+\delta_{cd})^{-\frac{1}{2}} - [(u_a u_b v_c v_d + v_a v_b u_c u_d) G(abdc;J) -$$

$$-(-1)^{j_c + j_d - J'} (u_a v_b u_c v_d + v_a u_b v_c u_d) F(abcd;J) + (-1)^{j_a + j_b + j_c + j_d - J - J} (u_a v_b v_c u_d + v_a u_b u_c v_d) F(abcd;J)], \tag{8}$$

with

$$G(abcd;J) = \sum_{m_a m_b m_c m_d} \langle j_a m_a j_b m_b | JM \rangle \langle j_c m_c j_d m_d | J'M' \rangle V^{pp}_{ab,cd}, \tag{9}$$

$$F(abcd;J) = \sum_{m_a m_b m_c m_d} \langle j_a m_a j_b m_b | JM \rangle \langle j_c m_c j_d m_d | J'M' \rangle V^{ph}_{ab,cd}. \tag{10}$$

$V^{pp}_{ab,cd}$ and $V^{ph}_{ab,cd}$ are matrix elements of particle-particle (pp) and particle-hole (ph) effective interaction, respectively. The ph matrix elements $V^{ph}_{ab,cd}$ is defined as [58, 59]

$$V^{ph}_{ab,cd} = -\sum_{J'} (2J'+1) \begin{Bmatrix} j_a & j_d & J' \\ j_c & j_b & J \end{Bmatrix} V^{pp}_{ad,cb}. \tag{11}$$

The moments can be obtained using the following equation,

$$m_k = \int E^k S(E)\, dE, \tag{12}$$

where $S(E)$ is the strength function [60]

$$S(E) = \sum_{\nu} \left| \langle \nu | \hat{F}_J | 0 \rangle \right|^2 \rho_\Gamma (E - E_\nu) \tag{13}$$

associated with the monopole operator where the Lorentzian function is defined as in the following:

$$\rho_\Gamma (E - E_\nu) = \frac{\Gamma}{2\pi} \frac{1}{(E - E_\nu)^2 + \left(\frac{\Gamma}{2}\right)^2} \tag{14}$$

with Γ is the smearing parameter.

Three ratios can be calculated using these different sum rules: the centroid energy, $E_{\text{cen}} = m_1 / m_0$, the constrained energy $E_{\text{con}} = \sqrt{m_1 / m_{-1}}$, and the scaling energy $E_{\text{s}} = \sqrt{m_3 / m_1}$, (where m_1 is the energy-weighted sum rule (EWSR), m_{-1} is the inverse EWSR, and m_3 is the cubic EWSR) [61].

3. Results and discussion

To study the ISGMR of the ^{92,94,96,98,100}Mo isotopes, the static HF+BCS equations were solved by using the Numerov method with the radial mesh size h = 0.1 fm within a model space based on ten Skyrme interaction sets, namely: KDE0v1 [40], eMSL08 [41], SKX [42], SGOI [43], v080 [44], SKP [45], SIV [46], SIII [47], SKIII [48], and SGI [43] of parameter sets presented in Table 1. The QRPA matrix diagonalization has been performed in the selected model space. The collective modes in nuclei provide very important information for understanding the structural and bulk properties of nuclear systems and their relation to the value of the incompressibility modulus K_{NM} of symmetric nuclear matter.

Table 1. **The nuclear matter incompressibility coefficient K_{NM} and the parameters of the used interactions**

Force	K_{NM}	t_0	t_1	t_2	t_3	x_0	x_1	x_2	x_3	W_0	α
KDE0v1	227.54	–2553.0843	411.6963	–419.8712	14603.6069	0.6483	–0.3472	–0.9268	0.9475	124.41	0.1673
eMSL08	229	–2429.09	493.72	–424.38	14502.7	0.334701	0.132739	–0.66643	0.337131	110.85	0.19196
SKX	271.06	–1445.3	246.9	–131.8	12103.9	0.34	0.58	0.127	0.03	148.6	1/2
SGOI	361.59	–1089	558.8	–83.7	8272	0.412	0	0	0	130	1
v080	231.17	–1827.96	251.271	–168.233	13419.5	0.528552	0.4	0.019271	0.483059	109.448	1/3
SKP	200.8	–2931.7	320.618	–337.409	18708.96	0.29215	0.65318	–0.53732	0.18103	100	0.167
SIV	324.55	–1205.6	765	–35	5000	0.5	0	0	1	150	1
SIII	356	–1128.75	395	–95	14000	0.45	0	0	1	120	1
SKIII	300	–1177	670	–49.7	11054	0.124	0	0	1	105	1
SGI	269	–1603	515.9	84.5	8000	–0.02	–0.5	–1.731	0.1381	115	1/3

3.1 Strength distribution

The calculations of the strength function EWSR/MeV for ^{92,94,96,98,100}Mo isotopes are compared to the experimental results [36, 62] in the long wavelength limit with smearing parameter Γ = 3 and 5 MeV. The general behavior of the experimental strength distribution is well described for most of the interactions, especially with Γ = 3 MeV. The equations of static HF+BCS were solved by using 10 Skyrme interactions. The E0 multipole distributions obtained for ^{92}Mo, ^{96}Mo, ^{94}Mo, ^{98}Mo, and ^{100}Mo are shown in Figs. 1 and 2. The calculated values are the sum rules of centroid energy E_{cen}, constrained energy E_{con}, and scaling energy E_s are illustrated in Table 2.

Table 2. **The calculated centroid energies, scaled energies, and constrained energies for ISGMR in ^{92,94,96,98,100}Mo are compared with the experiment**

Energy	Isotopes	Exp.	KDE0v1	eMSL08	SKX	SGOI	v080	SKP	SIV	SIII	SKIII	SGI
$E_{cen} = (m_1/m_0)$, MeV	^{92}Mo	$19.62^{+0.28}_{-0.19}$	18.104	17.564	19.883	22.526	18.186	14.674	24.648	22.268	18.182	19.528
	^{94}Mo	$17.57^{+1.14}_{-0.30}$	17.523	17.21	19.513	21.116	17.219	15.406	23.64	19.984	17.928	18.634
	^{96}Mo	$16.95^{+0.12}_{-0.10}$	17.133	16.943	18.77	20.177	16.59	15.079	22.936	20.109	17.743	18.03
	^{98}Mo	$16.01^{+0.19}_{-0.13}$	16.738	16.693	18.461	19.638	16.488	13.797	22.753	19.858	17.54	17.545
	^{100}Mo	$16.13^{+0.11}_{-0.10}$	16.859	16.366	18.228	20.306	16.325	14.454	22.255	19.725	16.761	17.124
$E_s = (m_3/m_1)^{1/2}$, MeV	^{92}Mo	$21.68^{+0.53}_{-0.33}$	18.728	18.181	20.746	23.562	19.075	16.808	25.565	23.372	19.098	20.228
	^{94}Mo	$19.62^{+3.54}_{-1.15}$	18.494	18.012	20.495	22.981	18.631	16.859	25.096	22.547	18.991	19.875
	^{96}Mo	$18.18^{+0.20}_{-0.13}$	18.269	17.844	20.116	22.503	18.29	16.665	24.741	22.327	18.896	19.575
	^{98}Mo	$17.29^{+0.46}_{-0.21}$	18.032	17.646	19.855	22.177	18.06	16.222	24.545	22.068	18.769	19.328
	^{100}Mo	$17.35^{+0.16}_{-0.12}$	18.025	17.425	19.625	22.339	17.815	16.121	24.284	21.881	18.306	19.109
$E_{con} = (m_1/m_{-1})^{1/2}$, MeV	^{92}Mo		18.015	17.483	19.745	22.318	17.952	13.853	24.479	22.049	18.001	19.414
	^{94}Mo	$17.06^{+0.75}_{-0.19}$	17.251	17.068	19.308	20.387	16.662	15.014	23.123	18.633	17.717	18.261
	^{96}Mo		16.797	16.747	18.268	19.246	15.836	14.604	22.181	19.299	17.525	17.526
	^{98}Mo		16.303	16.432	17.968	18.558	15.932	12.793	22	19.134	17.304	16.907
	^{100}Mo		16.577	16.09	17.755	19.684	15.872	13.928	21.476	19.068	16.261	16.318

The experimental and theoretical E0 distributions for Mo isotopes have been previously reported [35 - 38, 62]. Our calculated E0 strength distribution for ^{92,94,96,98,100}Mo isotopes and the experimental data are depicted in Figs. 1 and 2. Most of the E0 results are located between 10 and 35 MeV. Table 2 displays our calculated centroid energies m_1/m_0. The ISGMR strength distributions of these nuclei were fitted with a constrained combination of two peaks to account for the potential coupling of the ISGMR strength with the $J = 0$ component of the ISGQR [63 - 69].

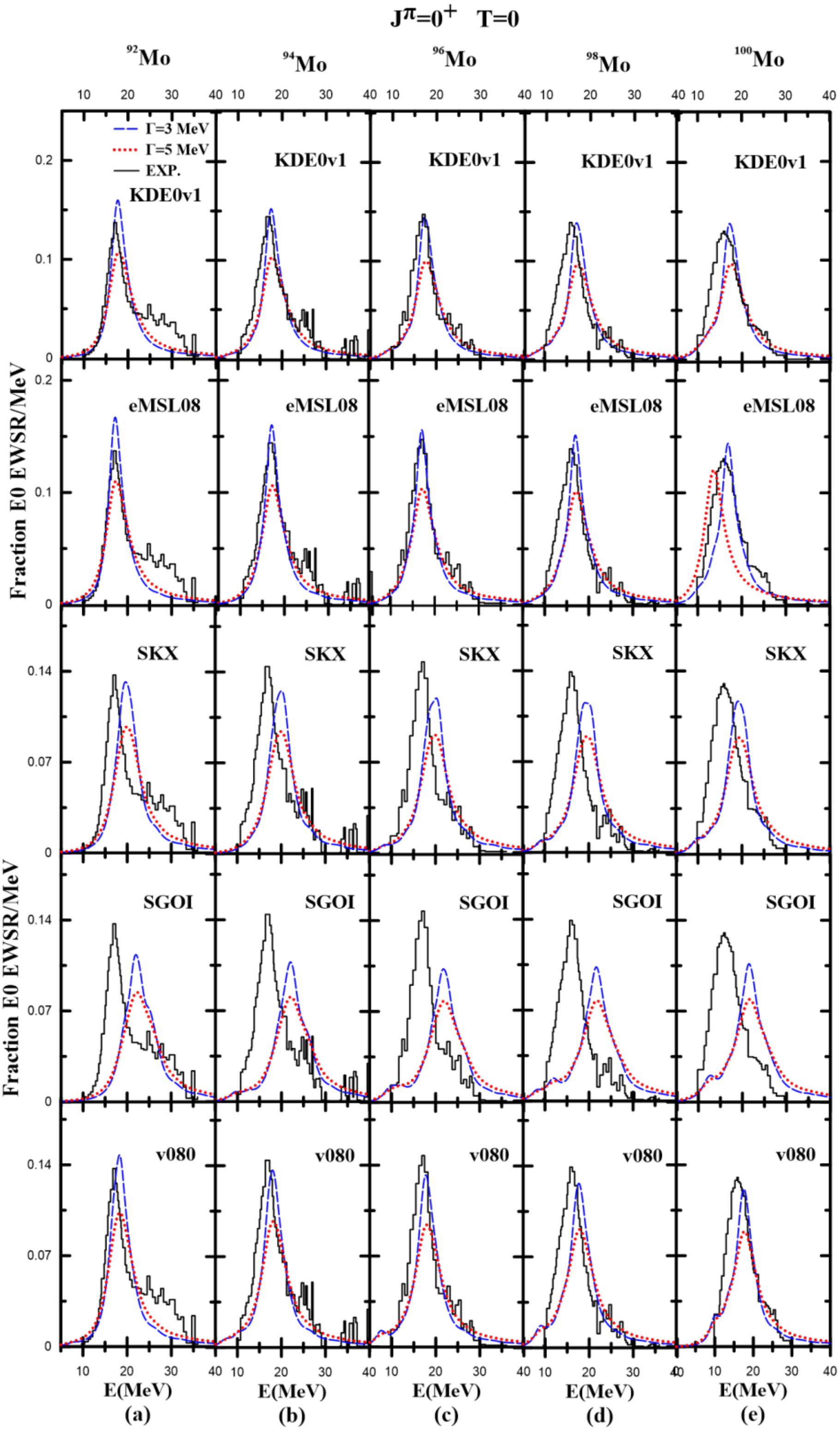

Fig. 1. Our calculated fraction EWSR/MeV of ISGMR E0 for (*a*) ^{92}Mo, (*b*) ^{94}Mo, (*c*) ^{96}Mo, (*d*) ^{98}Mo, (*e*) ^{100}Mo, using self-consistent HFBCS+QRPA with Skyrme interactions: KDE0v1, eMSL08, SKX, SGOI, and v080 compared with the experimental data [36, 62] (*black-solid lines*). Two Lorentzian smearing widths were used Γ = 3 MeV (*blue-dashed lines*) and 5 MeV (*red-dotted lines*). (See color Figure on the journal website.)

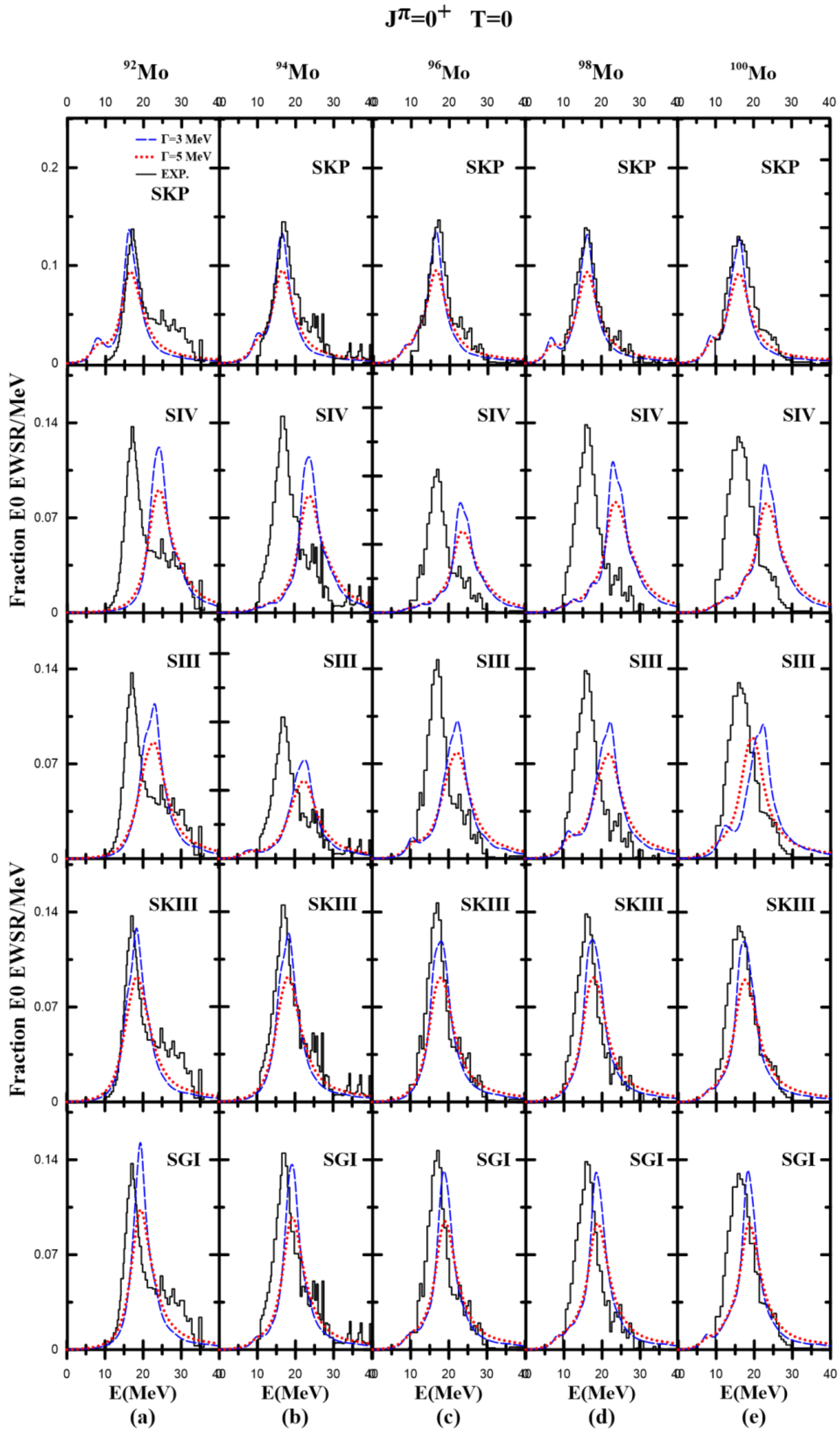

Fig. 2. Our calculated fraction EWSR/MeV of ISGMR E0 for (*a*) ^{92}Mo, (*b*) ^{94}Mo, (*c*) ^{96}Mo, (*d*) ^{98}Mo, (*e*) ^{100}Mo, using self-consistent HFBCS+QRPA with Skyrme interactions: SKP, SIV, SIII, SKIII, and SGI compared with the experimental data [36, 62] (*black-solid lines*). Two Lorentzian smearing widths were used Γ = 3 MeV (*blue-dashed lines*) and 5 MeV (*red-dotted lines*). (See color Figure on the journal website.)

In the study of ^{92}Mo in the earlier measurements [70, 71], just one peak was determined to be sufficient for the description of the ISGMR response; hence, in the discussion of all the studied isotopes going forward, we will only refer to the major ISGMR peak. The measured distribution of strength was extracted over the energy range $10 \le E_x \le 40$ MeV [66, 71, 72].

Our calculation consists of an approximately symmetrical peak between 16.5 and 24.5 MeV, with a tail extending up to 30 - 40 MeV, most interactions work best and agree with data concerning centroid energies, widths, and (smooth) profiles of strength. The GMR using KDE0v1, eMSL08, SKX, and SGI agree with data concerning peak high widths, and (smooth) profiles of strength. as shown in Fig. 1, *a* and Fig. 2, *a*.

In Fig. 1, *b* and Fig. 2, *b* the ISGMR of ^{94}Mo using KDE0v1, eMSL08, v080, and SKIII agree with data concerning height, widths, and (smooth) profiles of strength.

For ^{96}Mo, the strength distribution located a symmetrical peak between 15 and 23 MeV, extending up to 30 - 40 MeV, our calculated values with KDE0v1, eMSL08, and v080 agree with data concerning height, centroid energies, widths, and (smooth) profiles of strength as shown in Fig. 1, *c* and Fig. 2, *c*.

Our results of ^{98,100}Mo with the KDE0v1, eMSL08, and v080 agree with data concerning height, centroid energies, widths, and (smooth) profiles of strength as shown in Fig. 1, *d* and Fig. 2, *d* and in Fig. 1, *e* and Fig. 2, *e*.

The ratios E_{con}, $E_{cen,}$ and E_s were calculated from the extracted ISGMR peaks and are listed in Table 2, it is evident that the results for $^{92-96}$Mo for any given moment ratio are largely in agreement with one another. The centroid energies of E0 for the investigated Mo isotopes versus the mass number are plotted in Fig. 3, and we noted the decrease in the value of the E_{cen} with the increase in the value of A, besides the dependence on the value of K_{MN}, which will be discussed in the next section.

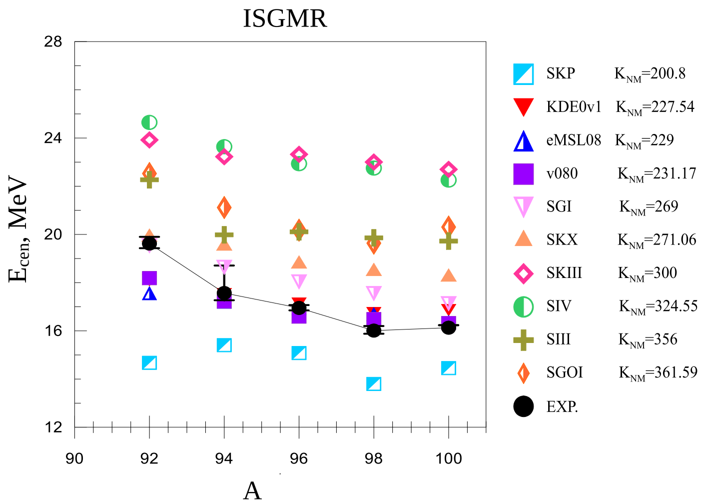

Fig. 3. Our calculated centroid energies of the E0 strength of the investigated Molybdenum isotopes using self-consistent HFBCS+QRPA with Skyrme interactions: KDE0v1, eMSL08, SKX, SGOI, v080, SKP, SIV, SIII, SKIII, and SGI in terms of atomic mass in comparison with experimental values (*black*) [36, 62]. (See color Figure on the journal website.)

3.2 The nuclear matter incompressibility coefficient K_{NM}

The available experimental data of centroid energies (delimited by the dashed lines) and our calculations of ^{92,94,96,98,100}Mo isotopes are depicted in Fig. 4 as a function of the nuclear matter incompressibility coefficient K_{NM} of the corresponding Skyrme interactions.

The E_{cen} for the investigated isotopes with KDE0v1 and v080 interactions of incompressibility coefficient between 229 and 231 MeV agrees with the experimental data. The result of the SKP is underestimated than the experimental value, while the calculated values with SIII, SIV, and SGOI Skyrme interactions are overestimated than the experimental value.

Overall, we see the well-known strong correlation between the E_{cen} and K_{NM} with Pearson linear correlation coefficients C ~ 0.87, 0.81, 0.834, 0.824, 0.844, respectively for ^{92}Mo, ^{94}Mo, ^{96}Mo, ^{98}Mo, ^{100}Mo.

4. Conclusions

The collective low-lying ISGMR with $\Gamma = 3$ MeV has a reasonable description provided by the self-consistent HFBCS+QRPA calculations with Skyrme interactions. Our results concerning height, width, and (smooth) profiles of strength are consistent with the measured strength distribution for the examined isotopes with Skyrme interaction of type KDE0v1 and eMSL08. The decrease in the value of the E_{cen} with the increase in the value of A, as well as the E_{cen} using interactions of K_{NM} between

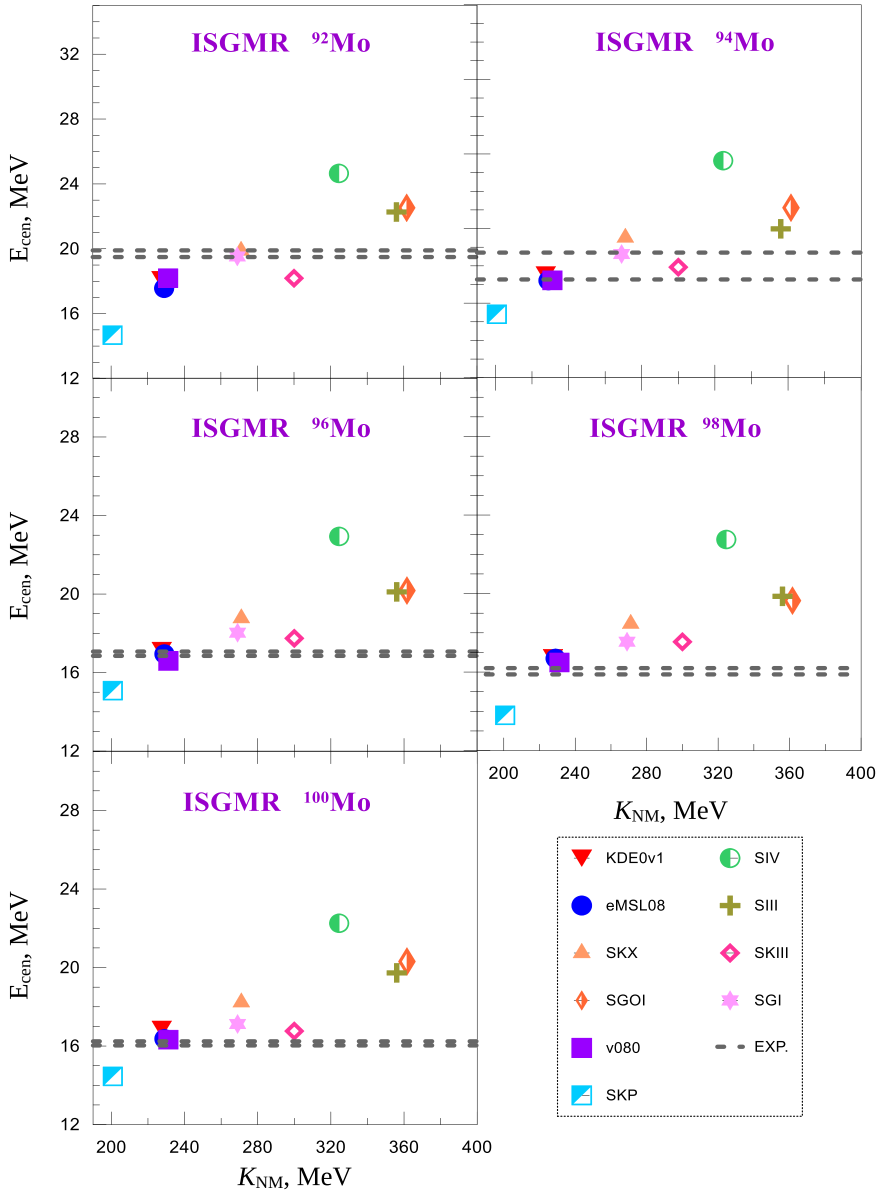

Fig. 4. Comparison of ISGMR experimental data [36, 62] of E_{cen} for ^{92,94,96,98,100}Mo, shown as the regions between the dashed gray lines, with our results (*colored symbols*). (See color Figure on the journal website.)

229 and 231 MeV agrees with the experimental data. Strong correlations between the E_{cen} and K_{NM} were obtained with Pearson linear correlation coefficients C ~ 0.87, 0.81, 0.834, 0.824, and 0.844, respectively for ^{92}Mo, ^{94}Mo, ^{96}Mo, ^{98}Mo, ^{100}Mo.

REFERENCES

1. N.V. Giai. Self-Consistent Description of Nuclear Excitations. Prog. Theor. Phys. Supp. 74-75 (1983) 330.
2. E. Khan, N.V. Giai. Low-lying 2^+ states in neutron-rich oxygen isotopes in quasiparticle random phase approximation. Phys. Lett. B 472 (2000) 253.
3. E. Khan et al. Low-lying collective states in neutron-rich oxygen isotopes via proton scattering. Phys. Lett. B 490 (2000) 45.
4. E. Khan et al. Proton scattering from the unstable nuclei ^{30}S and ^{34}Ar: structural evolution along the sulfur and argon isotopic chains. Nucl. Phys. A 694 (2001) 103.
5. J. Dobaczewski et al. Mean-field description of ground-state properties of drip-line nuclei: Pairing and continuum effects. Phys. Rev. C 53 (1996) 2809.
6. J. Engel et al. β decay rates of r-process waiting-point nuclei in a self-consistent approach. Phys. Rev. C 60 (1999) 014302.
7. M. Matsuo. Continuum Linear Response in Coordinate Space Hartree-Fock-Bogoliubov Formalism for Collective Excitations in Drip-line Nuclei. Nucl. Phys. A 696 (2001) 371.
8. E. Khan et al. Detecting bubbles in exotic nuclei. Nucl. Phys. A 800 (2008) 37.

9. O. Sorlin, M.-G. Porquet. Nuclear magic numbers: new features far from stability. Prog. Part. Nucl. Phys. 61 (2008) 602.
10. W.A. Mansour, A.H. Taqi. Isoscalar Giant Dipole Resonance of Tin Isotopes $^{112,\ 114,\ 116,\ 118,\ 120,\ 122,\ 124}$Sn Using HF-BCS and QRPA Approximations. Kirkuk J. Sci. 18(4) (2023) 42.
11. T. Li et al. Isotopic dependence of the giant monopole resonance in the even-A $^{112–124}$Sn isotopes and the asymmetry term in nuclear incompressibility. Phys. Rev. Lett. 99 (2007) 162503.
12. C. Monrozeau et al. First Measurement of the Giant Monopole and Quadrupole Resonances in a Short-Lived Nucleus: ^{56}Ni. Phys. Rev. Lett. 100 (2008) 042501.
13. T. Li et al. Isoscalar giant resonances in the Sn nuclei and implications for the asymmetry term in the nuclear-matter incompressibility. Phys. Rev. C 81 (2010) 034309.
14. D. Patel et al. Giant monopole resonance in even-A Cd isotopes, the asymmetry term in nuclear incompressibility, and the “softness” of Sn and Cd nuclei. Phys. Lett. B 718 (2012) 447.
15. J. Piekarewicz. Why is the equation of state for tin so soft? Phys. Rev. C 76 (2007) 031301(R).
16. J. Li, G. Colò, J. Meng. Microscopic linear response calculations based on the Skyrme functional plus the pairing contribution. Phys. Rev. C 78 (2008) 064304.
17. E. Khan. Role of superfluidity in nuclear incompressibilities. Phys. Rev. C 80 (2009) 011307(R).
18. P. Veselý et al. Giant monopole resonances and nuclear incompressibilities studied for the zero-range and separable pairing interactions. Phys. Rev. C 86 (2012) 024303.
19. E. Khan, J. Margueron, I. Vidaña, Constraining the Nuclear Equation of State at Subsaturation Densities. Phys. Rev. Lett. 109 (2012) 092501.
20. L.-G. Cao, H. Sagawa, G. Colò. Microscopic study of the isoscalar giant monopole resonance in Cd, Sn, and Pb isotopes. Phys. Rev. C 86 (2012) 054313.
21. L. Capelli, G. Colò, J. Li. Dielectric theorem within the Hartree-Fock-Bogoliubov framework. Phys. Rev. C 79 (2009) 054329.
22. E. Khan, N. Paar, D. Vretenar. Low-energy monopole strength in exotic nickel isotopes. Phys. Rev. C 84 (2011) 051301(R).
23. E. Khan et al. Incompressibility of finite fermionic systems: Stable and exotic atomic nuclei. Phys. Rev. C 87 (2013) 064311.
24. E. Yüksel, E. Khan, K. Bozkurt. The soft Giant Monopole Resonance as a probe of the spin-orbit splitting. Eur. Phys. J. A 49 (2013) 124.
25. J.P. Blaizot. Nuclear compressibilities. Phys. Rep. 64 (1980) 171.
26. J.P. Blaizot et al. Microscopic and macroscopic determinations of nuclear compressibility. Nucl. Phys. A 591 (1995) 435.
27. G.A. Mohammed, A.H. Taqi. Isoscalar Dipole Response in ^{92}Mo and ^{100}Mo Isotopes. Momento 67 (2023) 101.
28. S. Shlomo, V.M. Kolomietz, G. Colò. Deducing the nuclear-matter incompressibility coefficient from data on isoscalar compression modes. Eur. Phys. J. A 30 (2006) 23.
29. D.H. Youngblood, H.L. Clark, Y.-W. Lui. Incompressibility of Nuclear Matter from the Giant Monopole Resonance. Phys. Rev. Lett. 82 (1999) 691.
30. S. Shlomo, D.H. Youngblood. Nuclear matter compressibility from isoscalar giant monopole resonance. Phys. Rev. C 47 (1993) 529.
31. S.H. Amin, A.A. Al-Rubaiee, A.H. Taqi. Effect of Incompressibility and Symmetry Energy Density on Charge Distribution and Radii of Closed-Shell Nuclei. Kirkuk Journal of Science 17(3) (2022) 17.
32. D.R. Lide (Ed.). *CRC Handbook of Chemistry and Physics*. 87th ed. (CRC Press, 2006) 2608 p.
33. A. Moalem et al. Isotopic dependence of the giant quadrupole resonance in the stable even-mass molybdenum nuclei. Phys. Rev. C 20 (1979) 1593(R).
34. G. Duhamel et al. Inelastic alpha scattering to the giant quadrupole and monopole resonances of ^{58}Ni, ^{92}Mo, and ^{120}Sn at 152 MeV. Phys. Rev. C 38 (1988) 2509.
35. D.H. Youngblood et al. Unexpected characteristics of the isoscalar monopole resonance in the $A \approx 90$ region: Implications for nuclear incompressibility. Phys. Rev. C 88 (2013) 021301(R).
36. D.H. Youngblood et al. Isoscalar E0, E1, E2, and E3 strength in ^{92,96,98,100}Mo. Phys. Rev. C 92 (2015) 014318.
37. Krishichayan et al. Isoscalar giant resonances in ^{90,92,94}Zr. Phys. Rev. C 92 (2015) 044323.
38. K.B. Howard et al. Compressional-mode resonances in the molybdenum isotopes: Emergence of softness in open-shell nuclei near A = 90. Phys. Lett. B 807 (2020) 135608.
39. G. Colò et al. Isoscalar monopole and quadrupole modes in Mo isotopes: Microscopic analysis. Phys. Lett. B 811 (2020) 135940.
40. B.K. Agrawal, S. Shlomo, V. Kim Au. Determination of the parameters of a Skyrme type effective interaction using the simulated annealing approach. Phys. Rev. C 72 (2005) 014310.
41. Z. Zhfng, L.-W. Chen. Extended Skyrme interactions for nuclear matter, finite nuclei, and neutron stars. Phys. Rev. C 94 (2016) 064326.
42. B.A. Brown. New Skyrme interaction for normal and exotic nuclei. Phys. Rev. C 58 (1998) 220.
43. Q. Shen, Y. Han, H. Guo. Isospin dependent nucleon nucleus optical potential with Skyrme interactions. Phys. Rev. C 80 (2009) 024604.
44. J.M. Pearson, S. Goriely. Isovector effective mass in the Skyrme-Hartree-Fock method. Phys. Rev. C 64 (2001) 027301.
45. P.-G. Reinhard et al. Shape coexistence and the effective nucleon-nucleon interaction. Phys. Rev. C 60 (1999) 014316.
46. B.A. Brown et al. Neutron skin deduced from antiprotonic atom data. Phys. Rev. C 76 (2007) 034305.
47. H.S. Köhler. Skyrme force and the mass formula. Nucl. Phys. A 258 (1976) 301.

48. S. Krewald et al. On the use of Skyrme force in self-consistent RPA calculations. Nucl. Phys. A 281 (1977) 166.
49. T.H.R. Skyrme. The effective nuclear potential. Nucl. Phys. 9 (1958-1959) 615.
50. A.H. Taqi, M.S. Ali. Self-consistent Hartree-Fock RPA calculations in ^{208}Pb. Indian J. Phys. 92(1) (2018) 69.
51. J.R. Stone, P.-G. Reinhard. The Skyrme interaction in finite nuclei and nuclear matter. Prog. Part. Nucl. Phys. 58(2) (2007) 587.
52. D. Vautherin, D.M. Brink. Hartree-Fock calculations with Skyrme's interaction. I. Spherical Nuclei. Phys. Rev. C 5 (1972) 626.
53. M. Bender, P.-H. Heenen, P.-G. Reinhard. Self-consistent mean-field models for nuclear structure. Rev. Mod. Phys. 75 (2003) 121.
54. P. Ring, P. Schuck. *The Nuclear Many-Body Problem* (Heidelberg, Springer Berlin, 1980) 718 p.
55. E. Chabanat et al. A Skyrme parametrization from subnuclear to neutron star densities Part II. Nuclei far from stabilities. Nucl. Phys. A 635 (1998) 231.
56. W. Ryssens et al. Solution of the Skyrme-HF+BCS equation on a 3D mesh, II: A new version of the Ev8 code. Computer Physics Communications 187 (2015) 175.
57. D.J. Rowe. *Nuclear Collective Motion: Models and Theory* (London, Methuen, 1970) 340 p.
58. G. Colò et al. Self-consistent RPA calculations with Skyrme-type interactions: The skyrme_rpa program. Computer Physics Communications 184 (2013) 142.
59. A.H. Taqi, G.L. Alawi. Isoscalar giant resonance in ^{100,116,132}Sn isotopes using Skyrme HF-RPA. Nucl. Phys. A 983 (2019) 103.
60. A.H. Taqi, E.G. Khidher. Ground and transition properties of ^{40}Ca and ^{48}Ca nuclei. Nucl. Phys. At. Energy 19 (2018) 326.
61. S. Stringari. Sum rules for compression modes. Phys. Lett. B 108 (1982) 232.
62. J. Button et al. Isoscalar E0, E1, E2, and E3 strength in ^{94}Mo. Phys. Rev. C 94 (2016) 034315.
63. M. Itoh et al. Systematic study of $L \leq 3$ giant resonances in Sm isotopes via multipole decomposition analysis. Phys. Rev. C 68 (2003) 064602.
64. U. Garg et al. Splitting of the giant monopole resonance with deformation in Sm nuclei. Phys. Rev. Lett. 45 (1980) 1670.
65. S. Brandenburg et al. Fission decay of the isoscalar giant monopole resonance in ^{238}U. Phys. Rev. Lett. 49 (1982) 1687.
66. Y.K. Gupta et al. Splitting of ISGMR strength in the light-mass nucleus ^{24}Mg due to ground-state deformation. Phys. Lett. B 748 (2015) 343.
67. Y.K. Gupta et al. Deformation effects on isoscalar giant resonances in ^{24}Mg. Phys. Rev. C 93 (2016) 044324.
68. T. Peach et al. Effect of ground-state deformation on isoscalar giant resonances in ^{28}Si. Phys. Rev. C 93 (2016) 064325.
69. Y.K. Gupta et al. Isoscalar giant monopole, dipole, and quadrupole resonances in ^{90,92}Zr and ^{92}Mo. Phys. Rev. C 97 (2018) 064323.
70. Y.K. Gupta et al. Are there nuclear structure effects on the isoscalar giant monopole resonance and nuclear incompressibility near A ~ 90? Phys. Lett. B 760 (2016) 482.
71. M.N. Harakeh, A. van der Woude. Giant Resonances: Fundamental High-Frequency Modes of Nuclear Excitation (Oxford University Press, New York, 2001) 638 p.
72. B.K. Jennings, A.D. Jackson. Sum rules and the breathing mode. Nucl. Phys. A 342 (1980) 23.

А. Х. Такі*, Г. А. Мохаммед

Факультет фізики, Науковий коледж, Кіркукський університет, Кіркук, Ірак

*Відповідальний автор: alitaqi@uokirkuk.edu.iq

ІЗОСКАЛЯРНИЙ МОНОПОЛЬНИЙ ВІДГУК У НЕЙТРОННО-БАГАТИХ ІЗОТОПАХ МОЛІБДЕНУ З ВИКОРИСТАННЯМ САМОУЗГОДЖЕНОГО НАБЛИЖЕННЯ QRPA

Ізоскалярний гігантський монопольний резонанс (ISGMR) парних ізотопів молібдену ^{92,94,96,98,100}Mo вивчався в рамках самоузгодженого наближення Хартрі - Фока - Бардіна, Купера та Шріффера і квазічастинкового наближення випадкових фаз. У розрахунках використано десять наборів взаємодій типу Скірма з різними значеннями коефіцієнта нестисливості ядерної матерії K_{NM}. Розраховані розподіли сил, центроїдних енергій E_{cen}, ренормованих енергій E_s і обмежених енергій E_{con} в ISGMR порівнюються з наявними експериментальними даними. При відповідному значенні нестисливості ядерної матерії K_{NM} кілька типів взаємодій Скірма були успішними в описі розподілу сил ISGMR в ізотопах ^{92,94,96,98,100}Mo. У результаті було виявлено великі кореляції між E_{cen} і K_{NM}.

Ключові слова: розподіл сил, сили Скірма, наближення Хартрі - Фока - Бардіна - Купера - Шріффера, квазічастинкове наближення випадкових фаз.

Надійшла/Received 05.05.2023